OPTOELECTRONICS AND ADVANCED MATERIALS – RAPID COMMUNICATIONS Vol. 1, No. 7, July 2007, p. 329 - 332

Conduction mechanism in CdZnS thick films

D. PATIDAR*, N. S. SAXENA, KANANBALA SHARMA, T. P. SHARMA
Semi-conductor and Polymer Science Laboratory, 5-6, Vigyan Bhawan, Department of Physics, University of Rajasthan, Jaipur-302004, India

$Cd_{1-x}Zn_xS$ (x = 0, 0.2, 0.4, 0.6, 0.8 and 1) has been prepared by chemical method using cadmium chloride, zinc chloride and H_2S. The sintered films of $Cd_{1-x}Zn_xS$ have been deposited on the glass substrate using the screen-printing method. The crystal structure and composition of $Cd_{1-x}Zn_xS$ ternary sintered films have been determined by X-ray diffraction patterns. The electrical conductivity of these thin films has been determined using the Keithley Electrometer over the temperature range from room to 413 K. It is observed that the electrical conductivity decreases with increasing Zn concentration. The decrease in conductivity with increase of Zn concentration is attributed to the increase of grain boundary surface area, which is responsible for the decrease of carrier mobility. It is noticed that the lattice structure becomes more and more disordered with the increase of Zn content, which increases the grain boundary scattering. A non-linear increase of electrical conductivity at fixed Zn concentration with the increase of temperature is discussed.

(Received April 2, 2007; after revision May 22, 2007; accepted June 26, 2007)

Keywords: Screen-printing method; Sintering; Electrical conductivity; Grain boundary scattering

1. Introduction

The polycrystalline chalcogenide semi-conductors play an important role in solar cell due to their favourable electrical and optical properties. Among the chalcogenide semi-conductors, CdZnS is one of such type materials, which is an important materials for the development of various modern technologies of solid state devices such as solar cells, light emitting diode, detector etc. [1] because of lattice matching with absorber materials and band gap in visible reason.

CdZnS have been widely used as a wide band gap window material in heterojunction solar cells and in photoconductive devices. In solar cell system, CdS replaced by higher band gap ternary CdZnS has led to decrease in window absorption losses resulting an increase in the short circuit current in solar cell [2]. The CdZnS ternary compound is also potentially useful as a window material for fabrication of p-n junctions without lattice mismatch in the devices based an quaternary materials like $CuIn_xGa_{1-x}Se_2$ [3] and $CuIn(S_xSe_{1-x})_2$ [4].

In recent years major attention have been given to the investigation of electrical and optical properties of CdZnS in order to improve the performance of the devices and also for finding new applications. In this regard, an effort has been made to study the electrical properties of $Cd_{1-x}Zn_xS$ (x = 0, 0.2, 0.4, 0.6, 0.8 & 1) thick films, which is prepared by chemical method using cadmium chloride, zinc chloride & H_2S and explain the conduction mechanism in these films.

2. Experimental details

Samples of $Cd_{1-x}Zn_xS$ (x = 0, 0.2, 0.4, 0.6, 0.8 & 1) have been prepared by chemical method using cadmium chloride, zinc chloride & H_2S. In this method, an appropriate ratio of cadmium chloride and zinc chloride was taken in solution form (1 M). This solution was mixed thoroughly using magnetic stirrer for 20 minutes. H_2S gas produced from thiourea was then passed through this solution. From this reaction a precipitate of $Cd_{1-x}Zn_xS$ was obtained. The precipitate obtained was filtered and dried in open atmosphere. When the precipitate was completely dried, it was then crushed to fine powder by grinding in a mortar.

The thick films of $Cd_{1-x}Zn_xS$ (x = 0, 0.2, 0.4, 0.6, 0.8 and 1) have been prepared by the screen-printing method [5]. In this method, the paste of $Cd_{1-x}Zn_xS$ for screen printing were prepared by mixing the ratio 100:10 of chemically precipitated $Cd_{1-x}Zn_xS$ and zinc chloride (cadmium chloride for CdS) as a adhesive source with ethylene glycol as a binder. The paste was then screen printed through the polyester screen onto clean glass substrates. The screen-printed films thus prepared were dried at 373 K for two hours in an oven. The reason of drying the sample at lower temperature was to avoid the cracks in the samples. After this, the films were then sintered, at 673 K temperature for ten minutes in the furnace. The melting point of zinc chloride is 556 K, yet the removal of zinc chloride takes place at lower temperature. To obtain stable sintered films, organic material should not remain in the sample. As the removal of organic substance takes place at about 673 K, the sintering temperature cannot be less than 673 K.

3. Characterization

X-ray diffraction pattern gives the valuable information about the structure and composition of materials. The crystal structure and composition of

$Cd_{1-x}Zn_xS$ (x = 0, 0.2, 0.4, 0.6, 0.8 and 1) ternary sintered films have been determined by X-ray diffraction patterns applying Vegard's law using a Philips X-xay diffractometer with FeK_α radiation (λ = 1.93755 Å). Figs. 1-4 show the X-ray diffraction –patterns of sintered films of CdS, $Cd_{0.8}Zn_{0.2}S$, $Cd_{0.6}Zn_{0.4}S$ and ZnS, respectively. These XRD patterns confirm the formation and composition of the alloys of $Cd_{1-x}Zn_xS$ ternary system with x = 0, 0.2, 0.4, 0.6, 0.8 and 1. The presence of sharp structural peaks in these XRD patterns confirms the polycrystalline nature of the sintered films. The experimental d-values for the different composition of $Cd_{1-x}Zn_xS$ (x = 0, 0.2, 0.4, 0.6, 0.8 and 1) system are determined using the Bragg's relation [6] by taking the θ value from the peak position of XRD pattern. Some other sharp peaks observed in the vicinity of the main peaks are the K_β peaks. These d-values are compared with the d*-values (ASTM) obtained from Vegard's law for $Cd_{1-x}Zn_xS$ system. According to Vegard's law, the d*-values for ternary system will be linear function of concentration x in $Cd_{1-x}Zn_xS$. The experimental d-values and d*-values from ASTM data are in good agreement as shown in Table 1 and prove the hexagonal (wurtzite) structure for all composition of $Cd_{1-x}Zn_xS$.

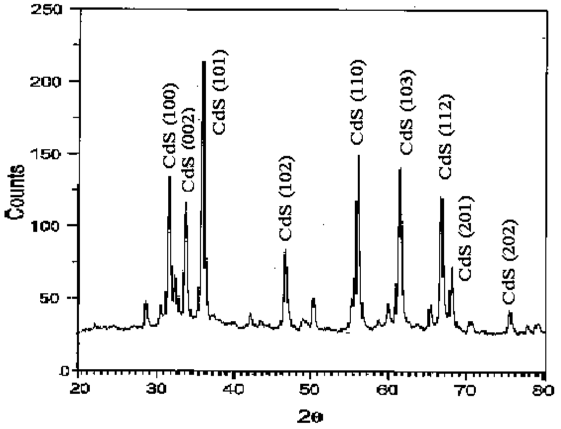

Fig. 1. XRD pattern of CdS.

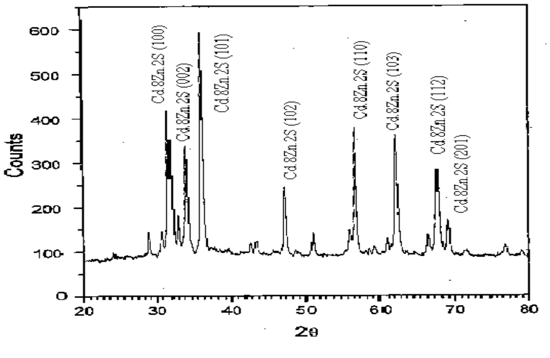

Fig. 2. XRD pattern of $Cd_{0.8}Zn_{0.2}S$.

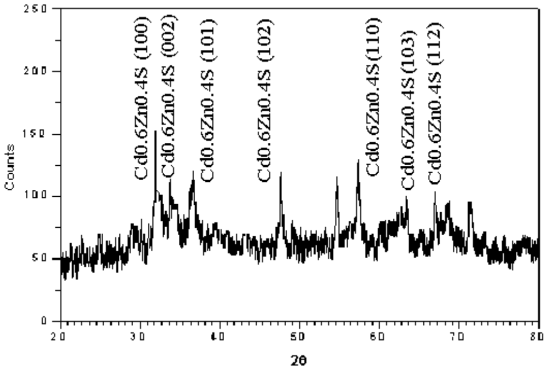

Fig. 3. XRD pattern of $Cd_{0.6}Zn_{0.4}S$.

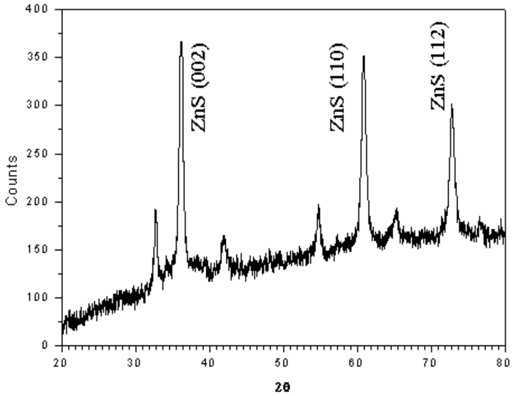

Fig. 4. XRD pattern of ZnS.

Table 1. X-ray diffraction data for CdS, $Cd_{0.8}Zn_{0.2}S$, $Cd_{0.6}Zn_{0.4}S$ and ZnS respectively.

S. No.	2θ	d=(λ/2Sin θ) (Å)	d* (Å)	Plane (hkl)
CdS				
1	31.416	3.578	3.583	(100)
2	33.541	3.357	3.357	(002)
3	35.817	3.150	3.160	(101)
4	46.374	2.460	2.450	(102)
5	56.00	2.064	2.068	(110)
6	61.311	1.900	1.898	(103)
7	66.774	1.760	1.761	(112)
8	68.140	1.729	1.731	(201)
9	75.728	1.578	1.584	(202)
$Cd_{0.8}Zn_{0.2}S$				
1	31.871	3.528	3.528	(100)
2	33.996	3.313	3.311	(002)
3	36.272	3.112	3.113	(101)
4	47.198	2.419	2.415	(102)
5	56.759	2.038	2.037	(110)
6	62.222	1.874	1.871	(103)
7	67.837	1.736	1.735	(112)
8	69.202	1.706	1.705	(201)

$Cd_{0.6}Zn_{0.4}S$				
1	32.645	3.447	3.473	(100)
2	34.488	3.268	3.265	(002)
3	36.727	3.075	3.066	(101)
4	48.082	2.378	2.379	(102)
5	57.629	2.010	2.005	(110)
6	63.490	1.841	1.844	(103)
7	68.971	1.711	1.709	(112)
ZnS				
1	36.036	3.132	3.128	(002)
2	60.780	1.915	1.911	(110)
3	72.775	1.633	1.630	(112)

4. Results and discussion

The electrical conductivity measurements of $Cd_{1-x}Zn_xS$ (x = 0, 0.2, 0.4, 0.6, 0.8 and 1) thick films have been performed over the temperature range from room to 413 K through the Keithley Electrometer/ High Resistance meter 6517 A. Two indium co-planer electrodes have been deposited on these films using the vacuum evaporation technique in the vacuum of 2×10^{-5} Torr for taking such measurements. The electrical conductivity in these films decrease with the increase of Zn concentration in CdS as shown in Fig. 5. The conductivity decreases from 10^{-3} to 10^{-6} S/cm at room temperature with the increase of Zn concentration. This decrease in the electrical conductivity can be attributed to the effect of grain size. The grain size of these films decreases with increasing Zn content. The smaller grain sizes, which increase the grain boundary surface area are responsible for the decrease of carrier mobility. The type of carriers found in CdZnS thin films are electrons [7]. It is observed that the carrier mobility and carrier density decrease with increasing Zn content in CdS [8], which is attributed to the increase of stacking fault density and misorientation of the crystallites [9]. It is also noticed that the inter-grain barrier height increases with increasing Zn concentration [10], which is caused by the lowering of grain size. The increase of Zn concentration in CdS makes the lattice structure more and more disordered, and this is responsible for the increase of grain boundary scattering and hence the carrier mobility and electrical conductivity are diminished.

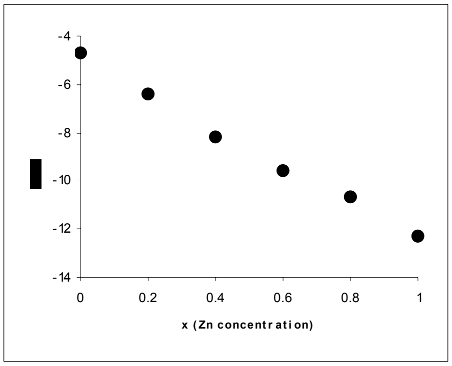

Fig. 5. Composition dependence of electrical conductivity of $Cd_{1-x}Zn_xS$ thick films.

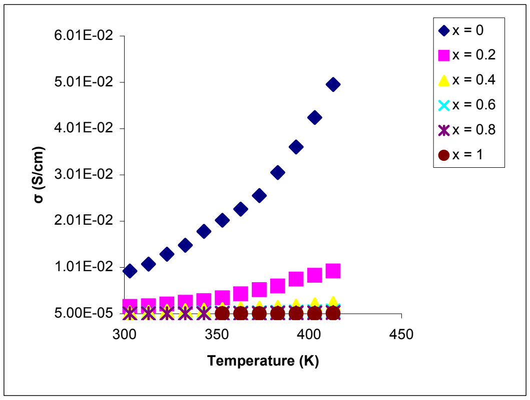

Fig. 6. The temperature dependence of electrical conductivity for different compositions of thick films of $Cd_{1-x}Zn_xS$.

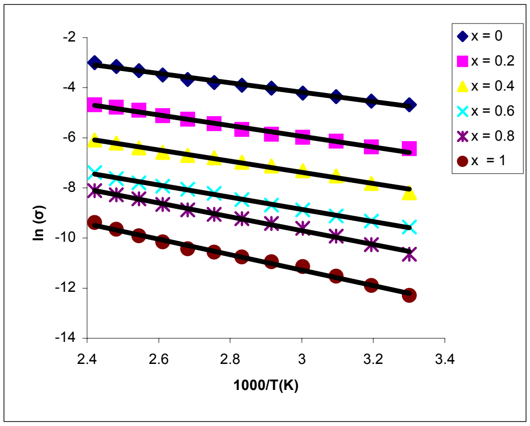

Fig. 7. Variation of ln(σ) versus 1000/T for different compositions of thick film of $Cd_{1-x}Zn_xS$.

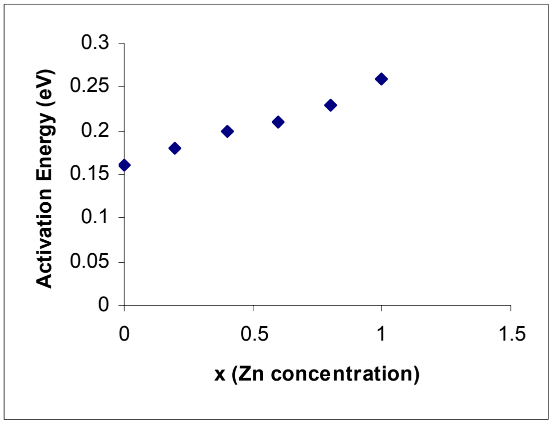

Fig. 8. Composition dependence of activation energy in $Cd_{1-x}Zn_xS$ thick films.

The temperature dependence of electrical conductivity (σ) of $Cd_{1-x}Zn_xS$ (x = 0, 0.2, 0.4, 0.6, 0.8 and 1) thick films with temperature is shown in Fig. 6. It is observed that conductivity increases non-linearly with increase of temperature for all compositions. This increase in conductivity can be explained on the basis of the growth of the grain size and increase in carrier density. The electrical conductivity depends on the structure of the films. It has been noticed that the thick films this prepared contain lattice defects and randomly oriented grains with the appearance of grain boundaries. An increase in temperature affects the structure of films due to the increase of grain size, removal of defects on the surface of films and decrease of grain boundary area. This can be attributed to the migration of smaller crystallites and joining of similarly oriented grains. This brings a decrease in scattering of electrons, which leads to an increase of mobility of charge carriers. It is also noticed that the carrier concentration increases with increase of temperature, which is responsible for the non-linear increase of conductivity with temperature. These sintered films follow an Arrhenius relationship in which the electrical conductivity is proportional to exp ($\Delta E_a/kT$), where ΔE_a is the activation energy of the electrical conduction. Fig. 7 shows the plot between ln(σ) and 1000/T for all the samples The activation energy has been determined using the slope of this figure for each composition. It is found that the activation energy of $Cd_{1-x}Zn_xS$ (x = 0, 0.2, 0.4, 0.6, 0.8 and 1) thick films increases almost linearly with increasing Zn concentration as shown in Fig. 8. An increase in the activation energy of $Cd_{1-x}Zn_xS$ (x = 0, 0.2, 0.4, 0.6, 0.8 and 1) thick films with the increasing concentration of Zn in CdS is suggestive of the fact that the conduction is due to thermally assisted tunneling of the charge carriers in the localized state, which are present in the band gap.

5. Conclusions

It is concluded that thick films of $Cd_{1-x}Zn_xS$ can be prepared using a simple method as discussed here. The electrical measurements reveal that the decrease of conductivity of $Cd_{1-x}Zn_xS$ with Zn concentration is due to the reduction of grain size and increase of disorder. Besides, a non-linear increase in the electrical conductivity with the increase of temperature is mainly due to the growth of grain size, removal of defects on the surface of the films and decrease of grain boundary area.

Acknowledgements

One of the authors, D. Patidar is grateful to DRDO, Govt. of India, New Delhi for providing Junior Research Fellowship. Authors would also like to thank to Mr. Vimal Kishore, Mr. Vibhav K. Saraswat, Mr. Neeraj Jain, Ms. Vinodini Shaktawat and Mrs. Rashmi Saxena for help in various ways.

References

[1] I. U. Oladegi, L. Chow, C.S.Ferekides, V. Viswanathan, Z. Zhao, Solar Energy Mate. Solar Cells **61**, 203 (2000).

[2] T. Yamaguchi, Y. Yamamoto, T. Tanaka, Y. Demizu, A. Yoshida, Thin Solid Films **281-282**, 375 (1996).

[3] T. Yamaguchi, J. Matsufusa, A. Yoshida, Jpn. J. Appl. Phys. **3**, L 703 (1992).

[4] T. Walter, M. Ruckh, K. O. velthaus, H. W. Schock, Proceedings of 11th EC Photovoltaic Solar Energy Conference p. 124 (1992).

[5] V. Kumar, V. Singh, S. K. Sharma, T. P Sharma, Optical Materials **11**, 29 (1998).

[6] B. D. Cullity, Elements of X-ray Diffraction, (Addison Wesley, Massachusetts/ London) (1959).

[7] N. Romeo, G. Sberveglieri, L. Tarricone, Appl. Phys. Lett. **32**, 807(1978).

[8] K. T. R. Reddy, P. J. Reddy, J. Phys. D: Appl. Phys. **25**, 1345 (1992).

[9] L. L. kazmerski, W. B. Berry, C. W. Allen, J. Appl. Phys. **43**, 3515 (1992).

[10] B. Metin, K. Refik, O. Mustafa, Turk J. Phys. **26**, 121 (2002).

---

*Corresponding author: dinupartidar@gmail.com